Linking fast and slow positive feedback loops creates an optimal bistable switch in cell signaling

Xiao-Peng Zhang, Zhang Cheng, Feng Liu,* and Wei Wang†
National Laboratory of Solid State Microstructure and Department of Physics, Nanjing University, Nanjing 210093, China
(Received 18 June 2007; revised manuscript received 21 August 2007; published 27 September 2007)

Interlinked positive feedback loops are frequently found in biological signaling pathways. It is intriguing to study the dynamics, functions, and robustness of these motifs. Using numerical simulations and theoretical analysis, here we explore the sensitiveness and robustness of positive feedback loops with various time scales. Both single and dual loops can behave as a bistable switch. We study the responses of five types of bistable switches to noisy stimuli. The noise-induced transitions between two states are discussed in detail by using energy landscape. The dual-time switch, consisting of interconnected fast and slow loops, is both sensitive to stimuli and resistant to fluctuations in stimulus. This provides a novel mechanism for creating optimal bistable switches and memory modules. Our results also suggest that the dual-time switch can act as a ubiquitous motif with sensitive robustness in biological systems.

DOI: 10.1103/PhysRevE.76.031924 PACS number(s): 87.16.Yc, 05.40.−a, 87.17.Aa

I. INTRODUCTION

The notion of feedback is one of the most fundamental concepts in cell signaling [1,2]. Signaling systems that include strong positive feedback have the potential to exhibit bistability and hysteresis [3,4]. A bistable system can alternate between two discrete steady states and convert continuous stimuli into discontinuous switchlike responses [5]. Bistability plays essential roles in important cellular processes such as differentiation [6–8] and cell cycle progression [9,10].

A single positive feedback loop with some ultrasensitivity is considered sufficient to act as a bistable switch [3,4,11]. However, multiple interconnected positive feedback loops are frequently found in subnetworks of large cellular and genetic networks [12–14], regulating such processes as Xenopus oocyte maturation [8], polarization of yeast cells [9], and calcium signaling in mammals [15]. An issue thus arises concerning why interlinked loops rather than single loops are exploited in such signaling networks. A recent study provides a clue [12]: connecting fast and slow positive feedback loops produces a dual-time switch, which can be rapidly inducible and robust to noise in stimulus. By contrast, a single fast or slow loop is separately responsible for the speed of switching and the stability of switches. Moreover, linking two loops of the same kind brings no overall advantage over having a single loop. But it is worth noting that the dual-loop switch in Ref. [12] operates in a monostable regime. Thus, it is interesting to explore whether interlinked loops can exhibit bistability and have performance advantages over single loops.

It is well known that there exists noise in biological systems due to environmental fluctuations and the inherent stochastic nature of biochemical processes [16]. Since small changes in stimulus can be amplified by positive feedback [17,18], noise may drive a bistable switch to undergo stochastic transitions between two steady states [11,16,19–21]. This may impose constraints on the bistable switch acting as a memory unit [3,4,7,22]. For example, cells have to "remember" that they are differentiated long after the differentiation stimulus has been withdrawn [7]. On the other hand, robustness is believed to be an essential property of biological organisms [23]. Thus, it is intriguing to investigate how to enhance the robustness of bistable switches through reducing noise-induced transitions.

Motivated by the above considerations, here we explore the sensitiveness and robustness of bistable switches by using numerical simulation and theoretical analysis. We construct models to describe the dynamics of both single and dual interlinked positive feedback loops, which can behave as a bistable switch. We study the responses of five types of bistable switches to noisy stimuli. Noise-induced transitions between two states are investigated in detail by using energy landscape. We find that the switch composed of interlinked fast and slow loops is both sensitive to stimuli and resistant to noise. This provides a novel mechanism for creating optimal bistable switches and may be of wide applicability in cell signaling. The paper is organized as follows. In Sec. II, mathematical models of single and dual loops are given. We describe the responses of five types of bistable switches to noisy stimuli in Sec. III. A discussion and conclusion are presented in Sec. IV.

II. MODEL

Because biochemical networks underlying cellular functions are far too complex, the analysis of networks, under some conditions, can be best achieved through mathematical modeling. In the present study, mathematic models are developed to describe the dynamics of both single and dual positive feedback loops. A coarse-grained level of description is adopted while neglecting molecular details.

We discuss two cases, respectively. In the case of a one-loop switch [Fig. 1(a)], a mutual activation of A and *output* comprises a positive feedback loop. This module is extracted from many realistic biological circuits. A signaling protein A' could be converted into an activated form A by a process catalyzed by a stimulus S. For example, the stimulus S could

*Corresponding author. fliu@nju.edu.cn
†Corresponding author. wangwei@nju.edu.cn

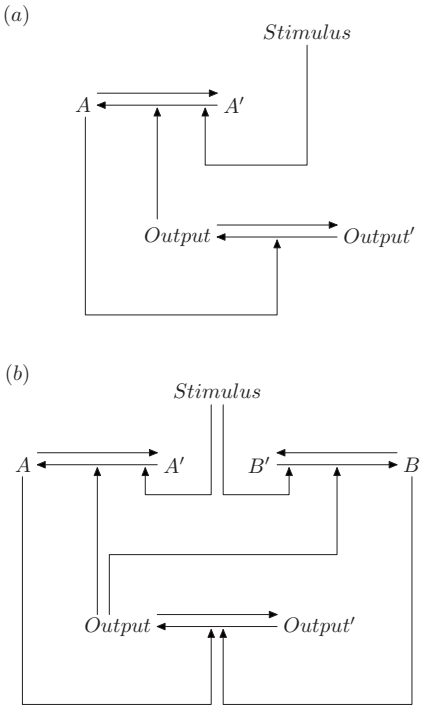

FIG. 1. Schematic illustration of the model. (a) The one-loop switch. A mutual activation of A and *output* comprises a positive feedback loop, and the activation of A is catalyzed by a stimulus. (b) The two-loop switch. A second loop is added through a mutual activation of B and *output*. The activation of B is also catalyzed by the stimulus.

be a kinase, and the conversion of A' to A could be due to phosphorylation. A could be converted back to A' through phosphatase. In the case of a two-loop switch [Fig. 1(b)], a second loop is introduced and both interact through a mutual activation of B and *output*. The dynamic equations for the one-loop and two-loop switches are similar to those in Ref. [12].

(i) One-loop switch

$$\frac{dC_{out}}{dt} = k_{on}C_A(1 - C_{out}) - k_{off}C_{out} + k_{out\text{-}min}, \quad (1)$$

$$\tau_A\frac{dC_A}{dt} = \left(k_1S + k_2\frac{C_{out}^n}{C_{out}^n + ec_{50}^n}\right)(1 - C_A) - C_A + k_{min}. \quad (2)$$

(ii) Two-loop switch

$$\frac{dC_{out}}{dt} = k_{on}(C_A + C_B)(1 - C_{out}) - k_{off}C_{out} + k_{out\text{-}min}, \quad (3)$$

$$\tau_A\frac{dC_A}{dt} = \left(k_1S + k_2\frac{C_{out}^n}{C_{out}^n + ec_{50}^n}\right)(1 - C_A) - C_A + k_{min}, \quad (4)$$

$$\tau_B\frac{dC_B}{dt} = \left(k_1S + k_2\frac{C_{out}^n}{C_{out}^n + ec_{50}^n}\right)(1 - C_B) - C_B + k_{min}. \quad (5)$$

Here all parameters and variables are dimensionless. C_A, C_B, and C_{out} represent the concentrations of the loop components, respectively, and S denotes the stimulus strength. τ_A (τ_B) is the time constant of the switch, determining its responsiveness. For the one-loop switch, we assume either fast (τ_A=2) or slow (τ_A=100) kinetics for the activation and inactivation of A. For the two-loop switch, we assume either fast kinetics for both the A and B loops, slow kinetics for both loops, or fast kinetics for the A loop and slow kinetics for the B loop. They are called the two-fast-loop, two-slow-loop, and dual-time switches, respectively.

It has been previously demonstrated that signaling cascades with ultrasensitive stimulus-response curves are important for converting gradual changes into all-or-none responses [3]. Here the positive feedback from *output* to A (B) is characterized by the Hill function, where the Hill coefficient n quantifies the ultrasensitivity. As we shall see, this can make switches more robust to fluctuations in stimulus.

The parameters are k_{on}=1, k_{off}=0.3, k_1=0.1, k_2=0.3, $k_{out\text{-}min}$=0.003, k_{min}=0.01, n=4, and ec_{50}=0.35 for the one-loop switch or 0.5 for the two-loop one. It is noted that we choose the values of parameters so that both the one-loop and two-loop switches can operate in a bistable regime. This is fundamentally different from the case in Ref. [12] where the two-loop switches act as monostable units. We have also tested other sets of parameter values and found that the conclusions drawn in this paper hold true provided that the loops act as bistable switches.

It is well known that cells operate in a noisy environment and that noise may interfere with cellular bistability. Here noise is introduced in the form of $S=S_0[1+\xi(t)]$. This is to model random fluctuations contained in the upstream signal. For simplicity, $\xi(t)$ is assumed to be Gaussian white with zero mean—i.e., $\langle\xi(t)\rangle=0$ and $\langle\xi(t)\xi(t')\rangle=2D\delta(t-t')$, where D is referred to as the noise intensity.

Numerical simulations of stochastic differential equations are carried out by using a second-order algorithm [24], and the integration time step is 0.01. We perform 1000 runs with different noise seeds for each experiment, and each run is to describe the dynamic behavior of one cell in a population of 1000 cells. Here we study the responses of five types of switches to noisy stimuli and explore their stability by analyzing distinct patterns of noise-induced transitions between two states. We also use energy landscapes to facilitate the study of noise effects.

III. RESULTS

A. Responses of switches to noise-free stimuli

We first study the responses of switches to noise-free stimuli. A system behaves as a bistable switch if it has two stable fixed points in the appropriate parameter regime. Figure 2(a) shows the bifurcation diagram for the one-loop switch as a function of S. The two saddle-node bifurcation points E and F enclose a bistable region. For any S within this region, the switch has two stable solutions and one unstable solution, which are represented by solid and dash-dotted lines, respectively. The switch therefore exhibits hysteresis, which is characteristic of bistable systems. When moving rightwards along the lower stable branch by increas-

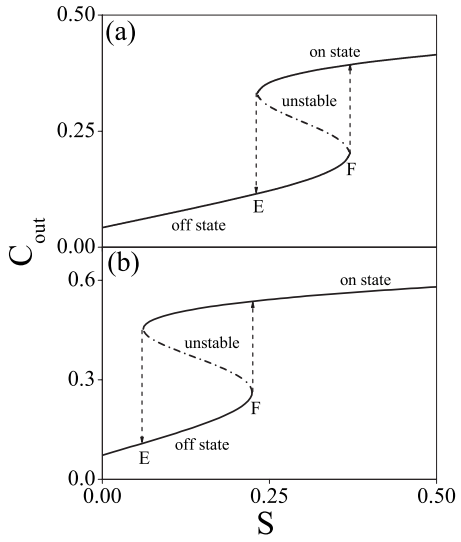

FIG. 2. Bifurcation diagram of output for (a) the one-loop switch and (b) the two-loop switch as a function of stimulus strength. Both switches exhibit bistability and hysteresis in the appropriate regime of S.

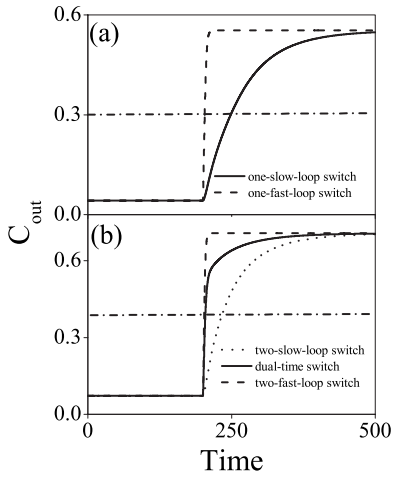

FIG. 3. Responses of switches to a step stimulus jumping from 0 to 3 at time $t=200$. (a) The one-loop switch with $\tau_A=100$ (solid line) or $\tau_A=2$ (dashed line); (b) the two-loop switch with $\tau_A=\tau_B=100$ (dotted line), or $\tau_A=\tau_B=2$ (dashed line), or $\tau_A=2$ and $\tau_B=100$ (solid line). The dash-dotted line indicates the midpoint between the initial and steady-state values of C_{out}.

ing S, C_{out} remains inactive until $S_F=0.371$. If S is further increased, the lower stable fixed point vanishes and the switch moves towards the upper stable branch, corresponding to an on state. If S is then decreased, the switch proceeds along the upper stable branch until $S_E=0.231$ and another transition occurs, bringing the switch back to the lower branch, an off state. Similar behavior is observed in Fig. 2(b) for the two-loop switch. It acts as a bistable switch when $0.061<S<0.224$. In contrast, the two-loop switches in Ref. [12] always operate in a monostable regime.

Hysteresis is of the potential importance in biological switching. First, it reduces the probability that a switch will repeatedly flip back and forth between two states when the stimulus is hovering near its threshold value [3]. Second, it provides a potential mechanism for biochemical memory. During the maturation of Xenopus oocyte, for example, the p42 MAPK/Cdc2 system can keep a long-term memory of a transient differentiation stimulus [7].

Sensitiveness and robustness are two important aspects when evaluating the performance of a bistable switch [25]. We illustrate the responses of five types of switches to a step stimulus in Fig. 3. Each switch is initially settled in an off state and then undergoes transition to an on state driven by the stimulus. We define response time t_r as the time required for C_{out} to reach the midpoint between its initial and steady-state values. The one-slow-loop switch turns on slowly with $t_r=47.2$, whereas the fast one flips simultaneously with $t_r=3.2$ [Fig. 3(a)]. Similar behavior is observed in Fig. 3(b) for the two-slow-loop (with $t_r=34.7$) and two-fast-loop (with $t_r=2.4$) switches. Obviously, the two-loop switches initiate slightly faster than the corresponding one-loop ones. In addition, the dual-time switch, consisting of interlinked fast and slow loops, still flips rapidly with $t_r=4.4$ because of the kinetic property of its fast loop. Thus, the fast loop is critical for the sensitiveness of switching. Robustness of the switches to fluctuations in stimulus will be investigated in the following.

B. One-loop switches

A bistable system always exhibits some degree of hysteresis, meaning that it is harder to flip the system from one state to the other than it is to maintain the system in its flipped state [3,4]. Under some conditions, however, stochastic effects can equilibrate the two states, reducing the potential of a switch for memory storage [11,22]. In this section, we explore noise-induced transitions between two states in the one-loop switch and their effect on the switch's stability.

We assume that a population of 1000 cells is simultaneously driven by $S(t)$ with the same S_0 and D but different noise seeds. Figure 4(a) illustrates the responses of three cells to the stimulus with $S_0=0.28$ and $D=0.8$. Note that $S_0=0.28$ is intermediate within the bistable regime [cf. Fig. 2(a)]. In the case of $\tau_A=2$, cells randomly switch back and forth between the on and off states. The time interval during which a cell resides in either of the two states also varies considerably among cells. Therefore, the one-fast-loop switch is destabilized in the presence of noise.

We can monitor the state of the population by computing a histogram of C_{out} at each moment. Figure 4(b) depicts time series of the histograms for two different initial conditions. Solid and dashed curves represent that all cells are initially settled in the lower and upper steady states for $S_0=0.28$ in the deterministic case, respectively. As time evolves, both histograms disperse around their initial distribution, widen and shorten, and change from unimodal to bimodal distributions. After a long period of time, two histograms converge to nearly the same bimodal distribution; that is, the final state is totally independent of its initial state. Thus, frequent transitions undermine the memory capability of the one-fast-loop switch.

To reveal the mechanism underlying noise-induced transitions and to quantify the stability of bistable switches, we introduce the concept of energy landscape [21,22]. Using a quasi-steady-state approximation, we set the right-hand side

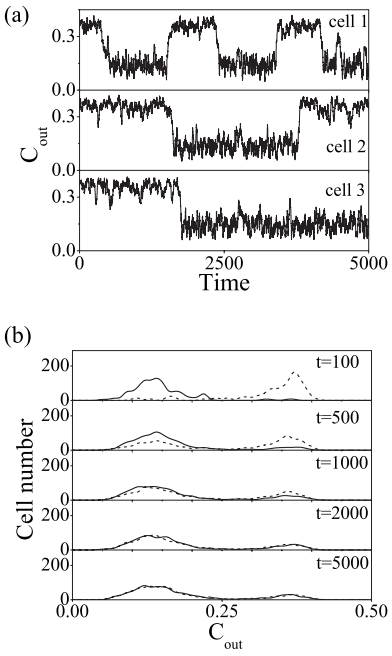

FIG. 4. Noise-induced transitions between two states of the one-fast-loop switch with $\tau_A=2$. $S_0=0.28$ and $D=0.8$. (a) The time courses of C_{out} for three cells. (b) The time series of the histogram of C_{out}, which depicts the distribution of C_{out} among a population of 1000 cells. Initially, all cells are settled in the off state (solid lines) or the on state (dashed lines).

of Eq. (2) to zero so that C_A is treated deterministically as a function of C_{out}. Then Eq. (1) can be rewritten in the form

$$\frac{dC_{out}}{dt} = \frac{1}{\tau}[f(C_{out}) + g(C_{out})\xi(t)], \tag{6}$$

$$f(C_{out}) = k_{on}\left(1 - \frac{1-k_{min}}{1 + k_1 S_0 + k_2 \dfrac{C_{out}^n}{C_{out}^n + ec_{50}^n}}\right) \times (1 - C_{out}) - k_{off} C_{out} + k_{out\text{-}min}, \tag{7}$$

$$g(C_{out}) = k_{on} \frac{k_1 S_0}{1 + k_1 S_0 + k_2 \dfrac{C_{out}^n}{C_{out}^n + ec_{50}^n}} (1 - C_{out}), \tag{8}$$

where τ is the effective time scale of the switch [26] and $\xi(t)$ is the noise term introduced in Eq. (2). The corresponding stochastic potential [27] is

$$\phi(C_{out}) = \tau \int^{C_{out}} \frac{f(C'_{out})}{g^2(C'_{out})} dC'_{out} + D \ln[g(C_{out})]. \tag{9}$$

Figure 5 displays the energy landscapes for different stimulus values. When S_0 is near either of the two threshold values (e.g., $S_0=0.24$), one steady state becomes metastable compared with the other [Figs. 5(a) and 5(c)]. For intermediate stimulus, the switch has a double-well potential [Figs. 5(b) and 5(d)]. Note the profound difference of scale on ordinate between the fast and slow switches. This will be exploited to interpret why the slow switch is more resistant to noise.

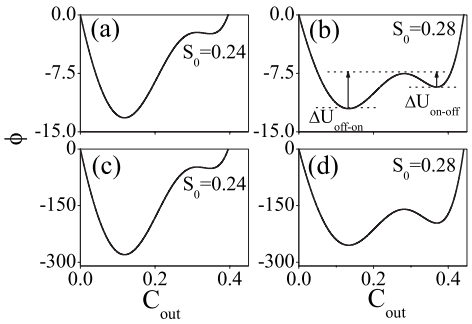

FIG. 5. The stochastic potential ϕ for the one-fast-loop (a), (b) and one-slow-loop (c), (d) switches. The stimulus is $S_0=0.24$ (a), (c) or 0.28 (b), (d).

The energy landscape provides an intuitive representation of the stability of a bistable switch. Minima in the landscape correspond to steady states separated by an energy barrier. The time evolution of C_{out} can be analogous to Brownian motion of an overdamped particle in an energy landscape. The effect of noise is to exert random kicks on the particle lying in one of these minima. On occasion, a series of kicks may drive the particle to escape from a local minimum and settle in a new valley. As we shall see, the transitions between two states can be described as an escape problem using Kramers rate theory [28]. That is, the switching rate satisfies the relationship

$$k_e \propto \exp\left(-\frac{\Delta U}{D}\right), \tag{10}$$

where ΔU represents an energy barrier and D the noise intensity. Thus, the larger the energy barrier, the more efficiently cells are trapped in the vicinity of steady states. According to Eq. (9), ΔU is proportional to the time scale τ in the weak noise limit. Since a large time scale leads to a small escape rate k_e, the slow switch must be more robust to noise than the fast one. Here there are two energy barriers: one for the transition from the on state to the off state, $\Delta U_{on\to off}$, and the other for the opposite transition $\Delta U_{off\to on}$.

Now we investigate the robustness of the one-loop switch to noise in terms of the above energy landscape. Suppose that all cells are in either of two steady states (initial state) and then some cells may flip to the other state (transition state) driven by noise. We define the ratio of the number of cells in the transition state to the number of all cells as the "fraction of transition" (F_t) at each moment.

We first study the case of the one-fast-loop switch with $\tau_A=2$. Figure 6(a) shows the time course of F_t for $S_0=0.24$. If all cells are initially settled in the on state, they are easily driven to the off state by weak noise. F_t rises quickly and equals 1 at steady state because $\Delta U_{on\to off}$ is sufficiently small. We calculate the switching rate and plot its natural logarithm versus $-\Delta U/D$ in the inset of Fig. 6(a). The points fall on a line with the slope close to one, implying that Kramers rate theory is a good approximation to describing noise-induced transitions. For $S_0=0.28$, stronger noise is

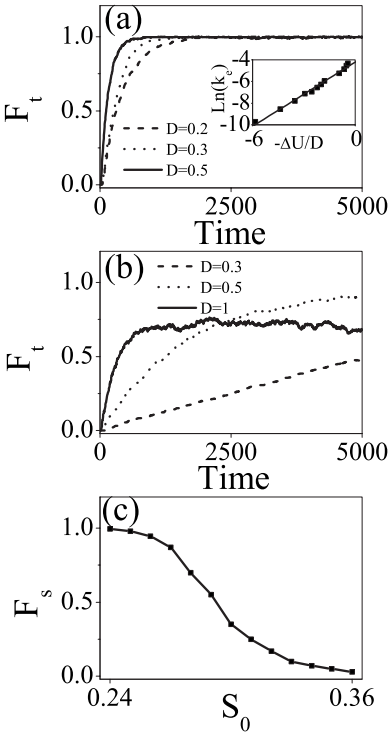

FIG. 6. The time course of F_t in the case of the one-fast-loop switch with $\tau_A=2$. (a) F_t vs time for $S_0=0.24$ and various noise intensities. The inset shows the natural logarithm of the switching rate vs $-\Delta U/D$. (b) F_t vs time for $S_0=0.28$ and various noise intensities. (c) The steady-state value of F_t vs S_0 for $D=1$.

needed to evoke stochastic transitions [Fig. 6(b)] because of an increment in $\Delta U_{on\to off}$. Moreover, cells can flip back and forth between two states because $\Delta U_{off\to on}$ and $\Delta U_{on\to off}$ are comparable. This effect becomes more marked with increasing D. The small jitters in the curve for $D=1$ also signify the presence of back and forth transitions [see also Fig. 4(a)]. Thus, F_t for $D=1$ is smaller than F_t for $D=0.5$ at steady state. But the switching rate still rises with increasing D.

Figure 6(c) depicts the steady-state value F_s of F_t versus S_0 for $D=1$. If all cells are initially in the on state, F_s decreases from 1 to 0 when S is increased from 0.24 to 0.36. When S_0 is near the lower threshold value, the off state is far more stable than the on state and almost all cells reside in the off state at steady state. In contrast, almost all cells are trapped in the on state when S_0 is close to the upper threshold value. For intermediate S_0, F_s decreases with S_0. Obviously, if all cells are initially in the off state, F_s varies in a complementary way to the above case.

Figure 7(a) shows F_t for the slow-loop switch with $\tau_A=100$. Even for $S_0=0.24$, only strong noise can make cells switch from the on state to off state and F_t assumes a small value even for $D=5$. It also takes a long time ($\gg 5000$) for F_t to reach a steady state. The switching rate is very small owing to the large time scale ($\tau=70$) of the switch. Moreover, $\Delta U_{off\to on}$ is about 65 times as large as $\Delta U_{on\to off}$. For $S_0=0.28$, there almost exist no flips over a wide range of noise intensity since all cells are trapped in the initial state (data not shown). Thus, the one-slow-loop switch is far more robust to noise than the fast one. This is also clearly seen in Fig. 7(b). Strong noise makes the fast switch unstable with frequent transitions, whereas the slow switch is fairly robust with few transitions. Note that for the fast switch, the steady-state value of F_t is smaller than 1 owing to back and forth transitions between two states.

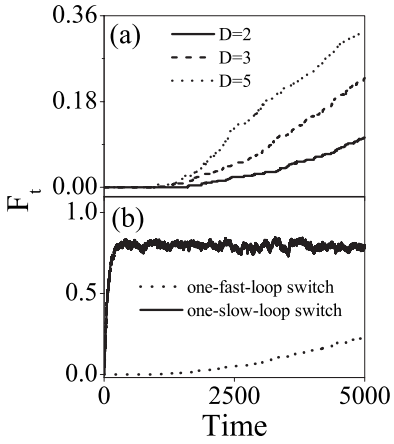

FIG. 7. (a) F_t vs time for $S_0=0.24$ and various noise intensities in the case of the one-slow-loop switch with $\tau_A=100$. (b) F_t vs time for $\tau_A=2$ (solid line) or $\tau_A=100$ (dotted line) with $S_0=0.24$ and $D=3$.

In addition, we can interpret the robustness of the slow switch to noise in terms of low-pass filtering. It has been suggested that transcriptional cascades can act as a low-pass filter rejecting transient fluctuations in input signal [29,30]. Through analyzing the frequency response of the switch to a "ZAP" signal that sweeps through many frequencies over time [31], we identify that the slow switch with large τ_A behaves like a low-pass filter (data not shown). Therefore, high-frequency components of white noise are filtered out by the slow switch and only its low-frequency components are available for evoking random transitions. This tends to reduce the switching frequency of the slow switch.

So far we have demonstrated that the one-fast-loop switch is sensitive to stimuli but unstable against noise, whereas the one-slow-loop switch is more robust to noise but slowly inducible. Therefore, to have an optimal bistable switch, we turn to explore the case of two-loop switch.

C. Two-loop switches

In this section, we investigate the condition under which a two-loop switch is both sensitive to stimuli and resistant to noise. We mainly study three types of switches: the two-fast-loop, two-slow-loop, and dual-time switches.

Using the same method as in the previous section, we obtain the stochastic potential ϕ for the two-loop switches, which is described as

$$\phi(C_{out}) = \tau \int^{C_{out}} \frac{f(C'_{out})}{g^2(C'_{out})} dC'_{out} + D \ln[g(C_{out})], \quad (11)$$

with

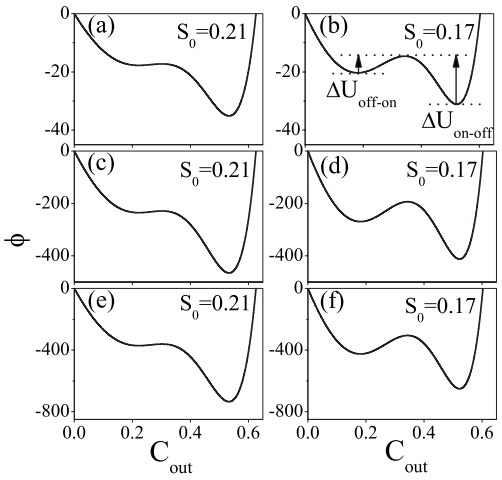

FIG. 8. The potential ϕ for the two-fast-loop switch (a), (b), dual-time switch (c), (d), and two-slow-loop switch (e), (f) in the weak noise limit. $S_0=0.21$ (a), (c), (e) or $S_0=0.17$ (b), (d), (f).

$$f(C_{out}) = 2k_{on}\left(1 - \frac{1-k_{min}}{1+k_1S_0+k_2\dfrac{C_{out}^n}{C_{out}^n+ec_{50}^n}}\right) \times (1-C_{out}) - k_{off}C_{out} + k_{out\text{-}min}, \quad (12)$$

$$g(C_{out}) = 2k_{on}\frac{k_1S_0}{1+k_1S_0+k_2\dfrac{C_{out}^n}{C_{out}^n+ec_{50}^n}}(1-C_{out}). \quad (13)$$

Figure 8 depicts the potential ϕ versus C_{out}, which exhibits a similar dependence on S_0 to that in Fig. 5. When S_0 is around either of the two threshold values, one steady state becomes metastable with respect to the other. ϕ displays a double-well structure when S_0 is intermediate within the bistable regime. Compared with Fig. 5, the scale on ordinate exhibits a more remarkable difference between three kinds of switches. Moreover, the energy barriers in the dual-time and two-slow-loop switches always assume great values except those corresponding to metastable states. This implies that these switches will be stable against noise when they are initially settled in the stable states.

We explore the stability of the switches by analyzing the time course of F_t and first study the case of the two-fast-loop switch with $\tau_A=\tau_B=2$. When S_0 is near the upper threshold value (0.224), even weak noise can drive cells from the off state to the on state, which makes F_t equal 1 at steady state [Fig. 9(a)]. This results from the lower energy barrier $\Delta U_{off\to on}$, which is due to the off state being metastable and the small effective time scale ($\tau=4.3$). Nevertheless, F_t rises relatively slowly for weaker noise since $\Delta U_{off\to on}$ is actually moderately small. Figure 9(b) displays F_t for $S_0=0.17$. Here the energy barrier $\Delta U_{off\to on}$ becomes larger compared with that for $S_0=0.21$ and thus cells can escape from the off state only in the presence of strong noise.

Figure 9(c) depicts the steady-state value F_s of F_t versus S_0. If all cells are initially in the off state, F_s rises sigmoidally from 0 to 1 when S_0 is increased from 0.07 to 0.21. The

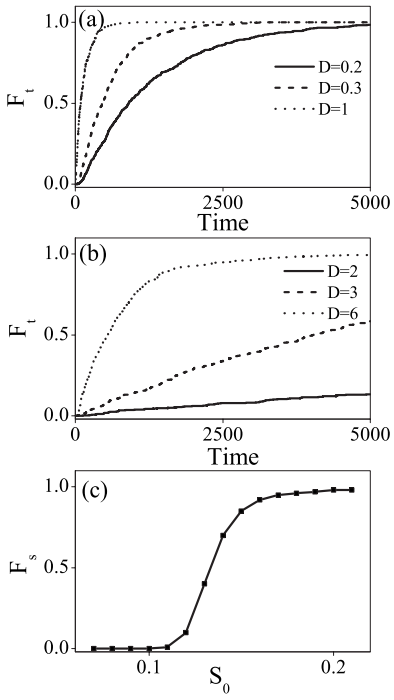

FIG. 9. The time course of F_t in the case of the two-fast-loop switch with $\tau_A=\tau_B=2$. F_t vs time for (a) $S_0=0.21$ and (b) $S_0=0.17$ with various noise intensities. (c) The steady-state value of F_t vs S_0 for $D=5$.

whole bistable regime can be divided into three ranges, over which F_s is around 0, significantly different from 1 or 0, and close to 1, respectively. In the first and third regimes, the two energy barriers differ drastically, and thus there are only one-way transitions between the two states even with high noise intensity (e.g., $D=5$). It is worth comparing Fig. 9(c) with Fig. 6(c). For the one-fast-loop switch, the second regime occupies about 50% of the bistable region (this regime may extend to the whole bistable region for higher noise intensity such as $D=5$). For the two-fast-loop switch, however, the second regime occupies only about 25% of the bistable region, while both the first and third regimes are enlarged. Such a difference mainly results from the fact that the energy barriers in the two-fast-loop switch assume slightly large values. Moreover, the existence of the third regime implies that linking two fast loops does not bring an overall performance advantage over having single fast loops.

Now we consider the other two types of two-loop switches. For the dual-time switch with $\tau_A=2$ and $\tau_B=100$, stronger noise can induce more transitions from the off state to the on state [Fig. 10(a)]. Compared with Fig. 9(a), F_t assumes a very small value and varies very slowly for $D=1$ since the switching rate becomes far smaller owing to the large effective time scale ($\tau=57$). For $S_0=0.17$, since both energy barriers are large enough, cells are trapped in their initial state and there are no transitions between two states over a wide range of noise intensities (data not shown). If we plot the steady-state value of F_t versus S_0 for $D=5$, the curve seems like a Heaviside function; i.e., F_t is 0 when $0.07 \le S_0 < 0.18$ and 1 for $0.18 \le S_0 \le 0.21$ (data not shown). Thus, the dual-time switch is more stable against noise than the two-fast-loop switch.

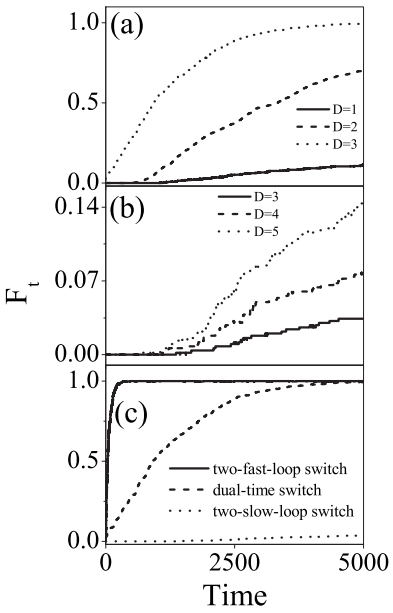

FIG. 10. F_t vs time for (a) the dual-time switch with $\tau_A=2$ and $\tau_B=100$ and (b) the two-slow-loop switch with $\tau_A=\tau_B=100$ with $S_0=0.21$ and various noise intensities. (c) F_t vs time for the two-fast-loop switch with $\tau_A=\tau_B=2$ (solid line), the dual-time switch (dashed line), and the two-slow-loop switch (dotted line) with $S_0=0.21$ and $D=3$.

The role of the slow loop in stabilizing the bistable switch is further demonstrated in the two-slow-loop switch. For $S_0=0.21$, it is so robust to noise that only very strong noise can drive cells from the off state to the on state [Fig. 10(b)]. F_t assumes a very small value and varies very slowly even for $D=5$. Here the effective time scale, $\tau=90$, is far larger than that for the two-fast-loop switch. We clearly see the distinct roles that the fast and slow loops play in bistable switches. The fast loop is critical for the speed of switching, whereas the slow loop is responsible for the stability of steady states by effectively decreasing switching rate. A direct comparison of the robustness of the three two-loop switches is made in Fig. 10(c), where the two-slow-loop and dual-time switches are more robust to fluctuations in stimulus than the two-fast-loop switch.

In addition, we plot F_t as a function of $1/\tau_A$ and $1/\tau_B$ in Fig. 11, where its value is represented by the grayscale intensity. In simulation, all cells are initially in the on state, and the value of F_t is calculated at time $t=5000$. We take the average of $F_t(\tau_B,\tau_A)$ and $F_t(\tau_A,\tau_B)$ to have better statistics. In the region corresponding to the two-slow-loop and dual-time switches (white-coded area), F_t is close to 0 with sparse switchings between two states. In contrast, in the region corresponding to two-fast-loop switches (black-coded area), F_t is close to 1 with nearly all cells flipping to the off state. This further indicates that the two-slow-loop and dual-time switches are much more resistant to noise than the two-fast-loop switch.

We have compared both the sensitiveness and robustness of three types of two-loop switches. The two-fast-loop switch is rapidly inducible but may undergo frequent transitions between two states driven by noise, whereas the two-slow-loop switch is resistant to noise but is slowly inducible. However, the dual-time switch exhibits a sensitive robustness [25], capable of yielding a fast yet robust response. Thus, the dual-time switch can be considered as an optimal bistable switch.

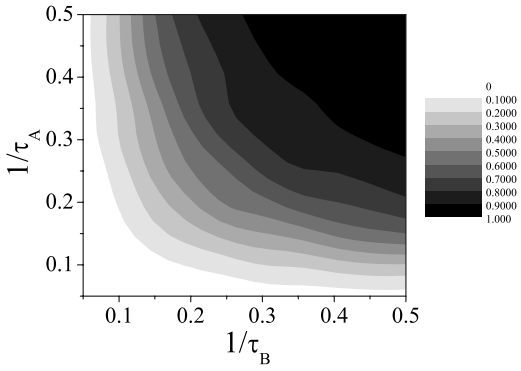

FIG. 11. F_t for the two-loop switch as a function of $1/\tau_A$ and $1/\tau_B$. F_t is calculated at time $t=5000$, and its value is represented by the grayscale intensity. $S_0=0.1$ and $D=5$.

IV. DISCUSSION AND CONCLUSION

We have demonstrated that both single and dual positive feedback loops can behave as bistable switches. The one-loop switch can assume either fast or slow dynamics. Linking two loops with various time scales can create the two-fast-loop, two-slow-loop, and dual-time switches, respectively. We have studied the responses of these switches to noisy stimuli, revealed the mechanism underlying stochastic transitions between two states, and analyzed the stability of switches by using energy landscape. The fast loop is responsible for the speed of switching between two states, while the slow loop is crucial for the stability of steady states. Thus, the dual-time switch is both sensitive to stimuli and resistant to noise. This suggests that linking fast and slow positive feedback loops can create an optimal bistable switch.

Bistability is extremely important in cell signaling. Bistable switches are able to convert a transient stimulus into a self-sustaining, irreversible response, providing a mechanism for epigenetic memory [32,33]. A positive-feedback-based memory module is widely exploited in cell fate decisions [3,4,7,22]. However, cellular processes are essentially stochastic and small fluctuations in stimulus could be amplified by positive feedback [17,18]. Noise-induced transitions may lead to false fate decision, which should be avoided by precise control [2].

How to make bistable switches both rapidly inducible and robust to fluctuations in stimulus is hence a challenging issue in cell signaling [25]. Our results may provide insight into this. Linking fast and slow loops is capable of establishing a fascinating harmony between sensitiveness and robustness. The fast loop makes a switch sensitive to deterministic change in stimulus, while the slow loop behaves like a low-pass filter and effectively reduces the switching frequency. It is noteworthy that the dual-time switch has been exploited as

a common building block in many signaling pathways [12–14]. The present work further elucidates why the dual-time switch is optimal and may act as a robust motif in signaling networks.

It is of interest to compare the present work with the previous study by Brandman *et al.* [12]. They illustrated the advantage of interlinked fast and slow positive feedback loops in cell signaling. More attention was focused on the speed of switching between two states and the fluctuations in output induced by noise. The two-loop switches operate in a monostable regime. In our work cellular switches exhibit bistability and hysteresis. We studied in detail dynamic behaviors of five types of bistable switches and emphasized the optimality of the dual-time switch. We found that the slow loop can effectively decrease the switching rates, which is of functional importance in cellular processes. In Xenopus oocyte maturation, for example, the slow feedback loop helps prevent the reversion of Cdc2 during the critical interkinesis period [8]. In budding yeast polarization, the presence of the actin-based slow loop may be important to reduce the flickering of the polarization switch [9].

In conclusion, the dual-time switch is both sensitive to stimuli and resistant to fluctuations in stimulus. It seems possible to act as a ubiquitous motif with sensitive robustness in biological systems. Our findings provide a novel mechanism for creating optimal bistable switches. It is intriguing for experimental biologists to synthesize a dual-time genetic switch and to verify our suggestion.

ACKNOWLEDGMENTS

This work is partly supported by the NNSF of China Grant No. 10604028 and the National Basic Research Program of China (973 Program) Grant No. 2007CB814806.

[1] B. N. Kholodenko, Nat. Rev. Mol. Cell Biol. **7**, 165 (2006).
[2] M. Freeman, Nature (London) **408**, 313 (2000).
[3] J. E. Ferrell and W. Xiong, Chaos **11**, 227 (2001).
[4] J. E. Ferrell, Curr. Opin. Cell Biol. **14**, 140 (2002).
[5] U. S. Bhalla and R. Iyengar, Science **283**, 381 (1999).
[6] J. E. Ferrell and E. M. Machleder, Science **280**, 895 (1998).
[7] W. Xiong and J. E. Ferrell, Nature (London) **426**, 460 (2003).
[8] A. Abrieu, M. Doree, and D. Fisher, J. Cell. Sci. **114**, 257 (2001).
[9] R. Wedlich-Soldner, S. C. Wai, T. Schmidt, and R. Li, J. Cell Biol. **166**, 889 (2004).
[10] J. R. Pomerening, E. D. Sontag, and J. E. Ferrell, Nat. Cell Biol. **5**, 346 (2003).
[11] A. Becskei, B. Seraphin, and L. Serrano, EMBO J. **20**, 2528 (2001).
[12] O. Brandman, J. E. Ferrell, R. Li, and T. Meyer, Science **310**, 496 (2005).
[13] S. Bornholdt, Science **310**, 449 (2005).
[14] T. Casci, Nat. Rev. Genet. **6**, 878 (2005).
[15] R. S. Lewis, Annu. Rev. Immunol. **19**, 497 (2001).
[16] C. V. Rao, D. M. Wol, and A. P. Arkin, Nature (London) **420**, 231 (2002).
[17] T. Shibata and K. Fujimoto, Proc. Natl. Acad. Sci. U.S.A. **102**, 331 (2005).
[18] M. Samoilov, S. Plyasunov, and A. P. Arkin, Proc. Natl. Acad. Sci. U.S.A. **102**, 2310 (2005).
[19] T. S. Gardner, C. R. Cantor, and J. J. Collins, Nature (London) **403**, 339 (2001).
[20] Q. Liu and Y. Jia, Phys. Rev. E **70**, 041907 (2004).
[21] J. Hasty, J. Pradines, M. Dolnik, and J. J. Collins, Proc. Natl. Acad. Sci. U.S.A. **97**, 2075 (2000).
[22] M. Acar, A. Becskei, and A. van Oudenaarden, Nature (London) **435**, 228 (2005).
[23] N. Barkai and S. Leibler, Nature (London) **387**, 913 (1997).
[24] J. Wilkie, Phys. Rev. E **70**, 017701 (2004).
[25] R. P. Araujo and L. A. Liotta, Curr. Opin. Cell Biol. **10**, 81 (2006).
[26] It seems impossible to derive an analytical formula for τ theoretically. With simulations, we find that τ is 3.3 for the one-fast-loop switch with $\tau_A=2$ and 70 for the slow one with $\tau_A=100$, respectively. In the case of the two-loop switch, τ is 4.3 for the two-fast-loop switch with $\tau_A=\tau_B=2$, 57 for the dual-time switch with $\tau_A=2$ and $\tau_B=100$, and 90 for the two-slow-loop switch with $\tau_A=\tau_B=100$, respectively.
[27] H. Risken, *The Fokker-Planck Equation* (Springer, Berlin, 1984).
[28] P. Hänggi, P. Talkner, and M. Borkovec, Rev. Mod. Phys. **62**, 251 (1990).
[29] S. S. Shen-Orr, R. Milo, S. Mangan, and U. Alon, Nat. Genet. **31**, 64 (2002).
[30] S. Hooshangi, S. Thiberge, and R. Weiss, Proc. Natl. Acad. Sci. U.S.A. **102**, 3581 (2005).
[31] B. Hutcheon and Y. Yarom, Trends Neurosci. **23**, 216 (2000).
[32] N. Yildirim, M. Santillan, D. Horike, and M. C. Mackey, Chaos **14**, 279 (2004).
[33] M. Laurent and N. Kellershohn, Trends Biochem. Sci. **24**, 418 (1999).